COMPUTER-AIDED CIVIL AND INFRASTRUCTURE ENGINEERING

Computer-Aided Civil and Infrastructure Engineering **28** (2013) 604–620

A Generalized Integrated Corridor Diversion Control Model for Freeway Incident Management

Yue Liu*, Peng Li & Kevin Wehner

Department of Civil Engineering and Mechanics, University of Wisconsin-Milwaukee, Milwaukee, WI, USA

&

Jie Yu

School of Control Science and Engineering, Shandong University, Jinan, Shandong Province, China

Abstract: *This article presents a generalized diversion control model for freeway incident management that is capable of concurrently optimizing the detour rates and arterial signal timings over multiple roadway corridor segments between the freeway and its neighboring arterial. To capture various operational complexities due to the interactions between multiple diversions, this study has developed an extended corridor traffic flow model and integrated it in the overall optimization process. A biobjective control model is developed to maximize the utilization of available corridor capacity while not significantly increasing the total time spent by travelers on the detour route to ensure their compliance to the routing guidance. Genetic algorithm integrated with the rolling time horizon approach is employed to solve the proposed model. Case studies with a stretch of the I-94 corridor westbound from downtown Milwaukee to Waukesha have demonstrated the potential of the developed model for use in nonrecurrent congestion management.*

1 INTRODUCTION

Traffic delays on urban freeways due to congestion have significantly undermined the efficiency and mobility of the highway systems in the United States. According to the literature, up to 60% of those delays are due to nonrecurrent traffic congestion caused by the reduced capacity and overwhelming demand on critical metropolitan corridors coupled with long incident durations. In such conditions, if proper diversion control strategies could be implemented in time, motorists can circumvent the congested segments by detouring through parallel arterials. To properly guide such operations, the responsible agency needs to detect the incident in a timely manner and implement effective strategies at all critical control points within the corridor system, including offramps and arterial intersections (Jiang and Adeli, 2003; Adeli and Ghosh-Dastidar, 2004; Duthie et al., 2011). Adeli and associates introduced the concept of wavelets into the field of transportation and developed innovative algorithms for automated detection of incidents in freeways with a high incident detection accuracy and low false alarm rate (Samant and Adeli, 2000, 2001). Subsequently, Karim and Adeli (2002, 2003) developed an incident detection algorithm using wavelet energy representation of traffic patterns for both urban and rural freeways. Their pioneering and visionary work laid the foundation for creation of an intelligent freeway system in the United States and elsewhere (Adeli and Karim 2005; Adeli and Jiang, 2009).

To contend with this vital operational issue, transportation professionals have proposed a variety of traffic diversion control and route guidance strategies, which may prioritize either system-optimal or user-optimal traffic conditions within the freeway corridor system. Responsive route guidance strategies (Messmer et al., 1994; Mammar et al., 1996) have been first proposed to provide guiding plans for traffic, based on current measurements from the surveillance system, without using mathematical models in real time. Most of those strategies are localized in nature, i.e., they only

*To whom correspondence should be addressed. E-mail: *liu28@uwm.edu*.

DOI: 10.1111/mice.12024

generate independent plans for each off-ramp or diversion point. Extending such simple responsive strategies, multivariable responsive strategies, as well as heuristics and advanced feedback control concepts, have been developed to address the low-sensitivity issue with respect to varying demands and driver compliance rates (Pavlis and Papageorgiou, 1999; Wang and Papageorgiou, 2000). Responsive route guidance strategies, though they have been shown to considerably reduce travel delays compared with the no-control case, are unlikely to achieve the system-optimal traffic state due to the local nature of their control. Also, these strategies cannot provide information about future traffic conditions under current route guidance settings, which may limit their applications in a large traffic corridor network.

As an extension to responsive strategies, predictive strategies (Messmer et al., 1998; Wang et al., 2002) have been proposed, which employ a dynamic network flow model to predict future traffic conditions under the current route guidance settings, based on the current traffic state, control inputs, and predicted future demands. Compared with responsive strategies alone, these methods are generally more robust and are preferable when the corridor network has long links. However, more research and field experience are needed to verify their applicability under different topological and traffic conditions, especially under nonrecurrent traffic congestion.

Another category of diversion control is called the iterative strategy, which runs a freeway network model in real time with a route guidance plan adjusting at each time interval to ensure the successful achievement of the control goal. Therefore, they are predictive in nature and may aim at achieving either the system-optimal or user-optimal condition. For the system-optimal case, a set of control formulations usually aims at minimizing a specific network performance index under the constraints of splitting rates at diversion points over a preset time horizon (Papageorgiou, 1990; Lafortune et al., 1993; Iftar, 1995; Messmer and Papageorgiou, 1995; Wie et al., 1995; Muñoz and Laval, 2006). On the other hand, several studies have also focused on establishing user-optimal conditions via iterative route guidance strategies (Mahmassani and Peeta, 1993; Wisten and Smith, 1997; Wang et al., 2001; Hooshdar and Adeli, 2004). A key procedure embedded in those strategies is to modify the path assignment or splitting rates appropriately to reduce travel time differences among all alternative routes, which are evaluated by iteratively running a simulation model over a given time horizon.

In the past two decades, researchers began to realize the benefits of integrating freeway traffic diversion with other control measures to maximize the corridor operational performance. Several studies have documented the benefits of ramp metering with diversion over the scenario with no metering controls. Nsour et al. (1992) investigated the impacts of freeway ramp metering, with and without diversion, on traffic flow. Their results suggested that with proper ramp metering control and coordinated arterial signal timings, the level of service for the entire corridor could be improved. However, their study ignored the interaction of traffic flow between freeway and surface streets. Similar investigation can also be found in Moreno-Banos et al. (1993). More advanced integrated diversion strategies have also been developed to generate optimal route guidance schemes combined with other control measures (Ben-Akiva et al., 2001; Kotsialos et al., 2002), to provide routing with reliability (Kaparias et al., 2007; Nie and Wu, 2010), and to consider real-world driver behavior patterns (Paz and Peeta, 2009). Advanced traffic flow modeling and analysis techniques were also developed for more efficient traffic assignment and management (Bhaskar et al., 2011; Szeto and Sumalee, 2011; Karoonsoontawong and Lin, 2011; Treiber et al., 2011; Putha et al., 2012).

In view of the impact of detour flows on arterial traffic, a handful of integrated control models for mixed freeway and urban corridor have been formulated to produce diversion strategies and arterial signal timing adjustment jointly rather than independently. Most of the research focuses on developing nonlinear optimization models for determination of various corridor control strategies either simultaneously or sequentially. Cremer and Schoof (1989) first formulated an integrated control model, in which a two-level optimization framework was proposed with the upper level for diversion optimization and the lower level for optimization of ramp metering, speed limit, and intersection signal timings. In their model, the control variables are not optimized concurrently and the coordination of signals on surface streets is not considered. Chang et al. (1993) presented a dynamic control model for a commuting corridor, including a freeway and parallel arterial. With the assumption that traffic diversion and route choice of all traffic demands were predictable, their approach features incorporating ramp metering and intersection signal timing variables into a single optimization model and solving it simultaneously in a system-optimal fashion.

To improve the computing efficiency, other methods have been proposed in the literature by either linearizing the network flow formulations or employing the rolling solution techniques. Papageorgiou (1995) developed a linear optimal-control model to design integrated control strategies for traffic corridors, including both motorways and signal-controlled urban roads based on the store-and-forward modeling philosophy. Wu and Chang (1999) formulated a linear programming system for integrated corridor control in which the

flow-density relation was approximated with a piecewise linear function to facilitate the use of a successive linear programming algorithm for global optimality. Van den Berg et al. (2001) proposed a model predictive control approach for mixed urban and freeway networks, based on the enhanced macroscopic traffic flow models in which traffic flow evolution on ramps has been explicitly captured. Liu and Chang (2011) have proposed an integrated diversion control model to determine the best diversion control strategy (i.e., diversion rates and corresponding signal retiming plans at the detour route) that yields the maximum utilization of corridor capacity. Their control model has effectively integrated a set of macroscopic traffic flow models that can precisely model and predict the traffic evolution along the freeway mainline, arterial link, and on–off ramps.

Despite the promising progress from those integrated diversion control models, only limited studies have been done regarding the multiroute diversion control, which can best demonstrate its effectiveness under the following two scenarios: (1) the impact of an incident quickly exceeds the boundaries of a single-segment corridor and spill back to its upstream ramps and (2) insufficient ramp and turning lane capacity. The effectiveness of detour operations is usually constrained by the available capacity at ramps and intersection turning lanes. Implementation of detour operations only for the incident segment may not be effective if the demand surge due to diversion results in a bottleneck at the ramps.

In response to the above research needs, this article develops a model for integrated diversion control of a multisegment corridor, in which multiple detour routes comprising several on-ramps, off-ramps, and several segments of parallel arterials are employed to coordinately divert traffic under incident conditions. The proposed model is designed to have the following operational features: (1) selecting a set of critical upstream off-ramps and downstream on-ramps for use in the detour operations within each control interval (i.e., the control boundaries) so as to assist traffic operators in better prioritizing the limited control resources; (2) capturing various operational complexities due to the interactions between multiple diversion decisions as well as their impacts on arterial traffic patterns in a dynamic control environment; (3) determining the dynamic diversion rates and detour destinations for traffic at upstream off-ramps to effectively utilize the available capacity in the parallel arterials; and (4) updating arterial signal timings to prevent the formation of local bottlenecks due to detour traffic.

This article is organized as follows. The next section will present an extended corridor network flow model that can capture the interactions among multiple detouring traffic flows and their impacts on the local arterial. Grounded on the above formulation, Section 3 illustrates the optimal diversion control model with the objectives of maximizing the utilization of corridor capacity and concurrently minimizing the total time of detour traffic. The model was solved with a genetic algorithm (GA)-based heuristic, and extensive analysis of a stretch of the I-94 corridor from downtown Milwaukee to Waukesha is summarized in Section 4. Concluding comments along with key findings are reported in the last section.

2 THE EXTENDED CORRIDOR MODEL

This section presents an integrated model to cover multiple segments of a corridor network. The model is expected to capture explicitly the evolution of multiroute detour traffic along the ramps and surface streets as well as the resulting local bottlenecks caused by the dramatic change in traffic demand levels and patterns due to diversion operations. Those unique modeling features, when properly integrated with the traditional freeway model, can more accurately and effectively set the control variables in the overall corridor optimization process.

2.1 Arterial dynamics

In modeling the arterial traffic dynamics, this study has employed a lane-group-based model to capture the interactions between multiple detouring traffic flows as well as their impacts on local arterial. The lane-group-based model has shown its effectiveness in modeling overflow and blockage situation in the arterials (Liu et al., 2008), and has been employed to design efficient arterial signal timings (Liu and Chang, 2011; Liu et al., 2011). In this study, the lane-group-based model is extended to incorporate the impacts of multiple detouring traffic flows heading to different downstream on-ramps in the parallel arterial. We decompose the flow on a link into arterial traffic subflow and the detour traffic subflows (see Figure 1). The number of upstream inflow vehicles to link i at time step k is given by

$$q_i^{\text{in}}[k] = \sum_{j\in\Gamma(i)} \overline{Q_{ji}}[k] + \sum_{\mu\in S_\mu^-} \sum_{j\in\Gamma(i)} Q_{ji}^{\mu}[k] \qquad (1)$$

where $\overline{Q_{ji}}[k]$ and $Q_{ji}^{\mu}[k]$ represent the actual number of vehicles departing from upstream link j to link i for arterial traffic and detour traffic heading to on-ramp μ, respectively; $\Gamma(i)$ is the set of upstream links of link i; S_μ^- is the set of on-ramps downstream of the incident location.

Then, the upstream arrival vehicles will propagate to the end of the queue with an average approaching speed $v_i[k]$ calculated by the speed–density function

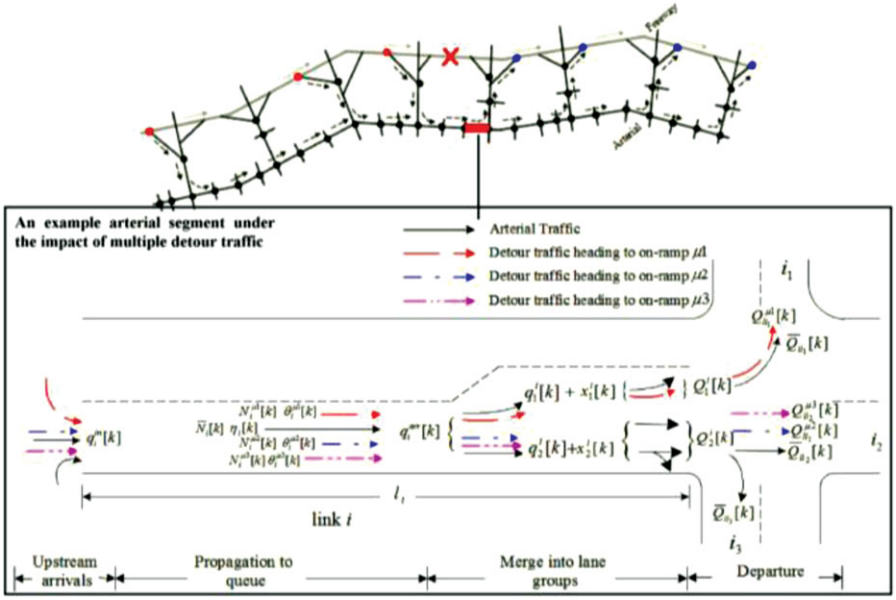

Fig. 1. Illustration of the interactions between multiple detouring traffic flows and their impacts on local arterial.

(Ben-Akiva, 2001); and the number of vehicles arriving at end of the queue of link i at time step k (see Figure 1) can be dynamically updated with:

$$q_i^{\text{arr}}[k] = \min\left\{\rho_i[k] \cdot v_i[k] n_i \cdot \Delta t, \overline{N_i}[k] + \sum_{\mu \in S_{\mu}^{-}} N_i^{\mu}[k] - x_i[k]\right\} \tag{2}$$

where $\rho_i[k]$ represents the running section density of link i at time step k; n_i is the number of lanes on link i; Δt is the update interval of the arterial systems; $\overline{N_i}[k]$ is the number of vehicles from normal arterial traffic on link i at time step k; $N_i^{\mu}[k]$ is the number of detour vehicles heading to downstream on-ramp μ on link i at time step k; and $x_i[k]$ is the number of vehicles in queue at link i at time step k.

After vehicles arrive at the end of the queue at a link, they will try to change lanes and merge into different lane groups based on their local and detour destinations. The number of vehicles that can actually merge into their destination lane group m at time step k is given by

$$q_m^i[k] = \min\left\{\max\left\{N_m^i - x_m^i[k], 0\right\}, \max\left\{q_m^{i,\text{pot}}[k] \times \left[1 - \sum_{m' \in S_i^M} \omega_{m'm}^i[k]\right], 0\right\}\right\} \tag{3}$$

where N_m^i is the storage capacity for lane group m; $x_m^i[k]$ is the queue length of lane group m on link i at time step k; therefore, $\max\left\{N_m^i - x_m^i[k], 0\right\}$ gives the available storage capacity in lane group m at time step k; S_i^M is the set of lane groups on link i; $\omega_{m'm}^i[k]$ is an element of the blocking matrix to model the discount of the merging capacity for lane group m due to the blockage from lane group m'. The blocking matrix concept is defined by Liu et al. (2008) to model the queue interactions among lane groups and will not be detailed here. Considering blockages from all possible lane groups, one can use $1 - \sum_{m' \in S_i^M} \omega_{m'm}^i[k]$ to represent the residual fraction of capacity to accommodate the potential number of vehicles that may merge into lane group m at time step k, given by Equation (4).

$$q_m^{i,\text{pot}}[k] = \tilde{x}_m^i[k] + \sum_{j \in \Gamma^{-1}(i)} q_i^{\text{arr}}[k] \cdot \left[\eta_i[k] \cdot \overline{\gamma_{ij}}[k] + \sum_{\mu \in S_{\mu}^{-}} (1 - \eta_i[k]) \cdot \theta_i^{\mu}[k] \cdot \gamma_{ij}^{\mu}\right] \cdot \delta_m^{ij} \tag{4}$$

Note that in Equation (4), $\tilde{x}_m^i[k]$ is the number of arrival vehicles with destination to lane group m queued outside the approach lanes due to blockage at link i at step k; $\eta_i[k]$ is the fraction of normal arterial traffic in total traffic at link i at step k; $\overline{\gamma_{ij}}[k]$ is the relative turning proportion of normal arterial traffic from link i to j; and then $\eta_i[k] \cdot \overline{\gamma_{ij}}[k]$ represents the percentage of normal arterial traffic flow going to link j at time step k;

$\theta_i^{\mu}[k]$ is the fraction of traffic heading to downstream on-ramp μ within the total detour traffic at time step k; γ_{ij}^{μ} is a binary value indicating whether detour traffic at link i heading to downstream on-ramp μ will use downstream link j or not; therefore, $\sum_{\mu \in S_{\mu}^{-}}(1-\eta_i[k]) \cdot \theta_i^{\mu}[k] \cdot \gamma_{ij}^{\mu}$ denotes the total percentage of detour traffic flow going to link j at time step k; δ_m^{ij} is a binary value indicating whether traffic going from link i to j uses lane group m. Hence, the total number of arriving vehicles to lane group m can be calculated with $\sum_{j \in \Gamma^{-1}(i)} q_i^{\text{arr}}[k] \cdot [\eta_i[k] \cdot \overline{\gamma_{ij}}[k] + \sum_{\mu \in S_{\mu}^{-}}(1-\eta_i[k]) \cdot \theta_i^{\mu}[k] \cdot \gamma_{ij}^{\mu}] \cdot \delta_m^{ij}$, which is added to $\tilde{x}_m^i[k]$ to reach $q_m^{i,\text{pot}}[k]$.

Both arterial and detour traffic will then depart from link i to downstream links. Due to the signal operation and the limitation of storage capacity in the downstream links, the actual number of vehicles departing from link i to j at time step k is given by

$$Q_{ij}[k] = \min\left\{ Q_{ij}^{\text{pot}}[k], \frac{Q_{ij}^{\text{pot}}[k]}{\sum_{i \in \Gamma(j)} Q_{ij}^{\text{pot}}[k]} \cdot s_j[k] \right\} \tag{5}$$

where $s_j[k]$ is the available space in link j at time step k and $\frac{Q_{ij}^{\text{pot}}[k]}{\sum_{i \in \Gamma(j)} Q_{ij}^{\text{pot}}[k]}$ is the proportion of the available space in link j allocated to accommodate flows from link i; $Q_{ij}^{\text{pot}}[k]$ is the number of vehicles potentially departing from link i to j at time step k, given by

$$Q_{ij}^{\text{pot}}[k] = \sum_{m \in S_i^M} \min\left\{ q_m^i[k] + x_m^i[k], Q_m^i \cdot \Delta t \times g^{np}[k] \right\} \cdot \lambda_m^{ij}[k] \tag{6}$$

where Q_m^i is the discharge capacity for lane group m; $g^{np}[k]$ is a binary value indicating whether signal phase p of intersection n is set to green at step k; $\min\left\{q_m^i[k] + x_m^i[k], Q_m^i \cdot \Delta t \cdot g^{np}[k]\right\}$ depicts the number of vehicles potentially departing from lane group m at time step k; $\lambda_m^{ij}[k]$ is the percentage of traffic in lane group m going from link i to j, which can be estimated with:

$$\lambda_m^{ij}[k] = \frac{\delta_m^{ij} \cdot \left[\eta_i[k]\overline{\gamma_{ij}}[k] + \sum_{\mu \in S_{\mu}^{-}} (1-\eta_i[k])\theta_i^{\mu}[k]\gamma_{ij}^{\mu} \right]}{\sum_{j \in \Gamma^{-1}(i)} \delta_m^{ij} \cdot \left[\eta_i[k]\overline{\gamma_{ij}}[k] + \sum_{\mu \in S_{\mu}^{-}} (1-\eta_i[k])\theta_i^{\mu}[k]\gamma_{ij}^{\mu} \right]} \tag{7}$$

Based on the above estimation of the arrivals and departures, key traffic state variables in an arterial link can be updated following the flow conservation law (Liu et al., 2011).

2.2 Freeway and ramps

A macroscopic traffic flow model was employed in this study to capture the traffic evolution for the freeway section. Detailed explanation of the model can be found in Messer and Papageorgiou (1990) and will not be detailed in this article. To accommodate the impact of merging and diversion behaviors due to traffic-obstructing incidents, we have further added the following terms in the speed evolution function of the original model:

$$-\frac{\phi \cdot \Delta T}{l_i} \cdot \frac{(n_i - n_{i+1})}{n_i} \cdot \frac{\rho_i[t]}{\rho_i^{cr} n_i} v_i^2[t] - \frac{\varphi \cdot \eta \cdot \Delta T}{\tau \cdot l_i} \cdot \frac{q_v[t]}{q_i[t] + q_{\mu}[t]} \cdot \frac{\rho_i^v[t] - \rho_{i+1}[t]}{\rho_i[t] + n_i \kappa} \tag{8}$$

where ΔT is the update interval of the freeway systems; t is the update time index for the freeway system ($t = k \cdot \Delta t / \Delta T$); n_i represents the number of lanes at section i; l_i is the length of section i; $\rho_i[t]$ is the density of section i at time step t; ρ_i^{cr} is the critical density of section i; $v_i[t]$ is the space mean speed in section i at time step t; $q_i[t]$ is the flow rate leaving section i, $q_v[t]$ is the flow rate leaving off-ramp v, and $q_{\mu}[t]$ is the flow rate entering from on-ramp μ at time step t; $\rho_i^v[t]$ is the density of off-ramp v at time step t; and $\phi, \varphi, \eta, \tau, \kappa$ are model parameters to be calibrated.

As on-ramps and off-ramps function to exchange diversion flows between the freeway and arterial system, this study has employed the lane-group-based concept to model on-ramps and off-ramps so that the freeway and arterial traffic dynamics can be connected into an overall corridor model. As illustrated in Figure 2, the on-ramp can be modeled as a simplified arterial link with only one lane group and one downstream link, while the off-ramp could also be modeled as an arterial link if the upstream arrival process is modified properly (Liu et al., 2011).

2.3 Data needs for the corridor model

For real-world application of the proposed corridor model, traffic states from the surveillance system must be properly estimated and projected in real time to provide feedback to the optimization model to update control strategies. The critical traffic state variables that need to be estimated or predicted in real time include density distribution, traffic flow rates, queue length distribution, turning fractions at intersections, and driver compliance rates.

There are many effective approaches in the literature for real-time identification of traffic flows and density distribution, based on online traffic measurements. The recent advances in traffic sensor technologies have

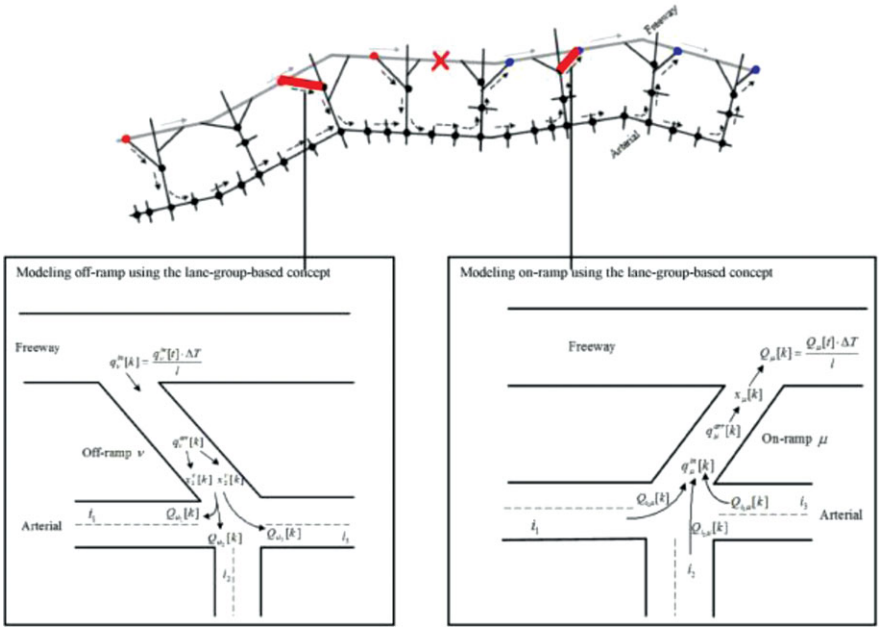

Fig. 2. Traffic flow dynamics at on-ramps and off-ramps.

also provided reliable tracking of queue evolution at an individual-movement level (Smadi et al., 2006). For turning fractions, Section 2.1 has proposed a corridor-wide approach to project the impact of detoured traffic on arterial turning movements, from which the composite turning proportion can be estimated or predicted as follows:

$$\gamma_{ij}[k] = \frac{\overline{Q_{ij}}[k] + \sum_{\mu \in S_\mu^-} Q_{ij}^{\mu}[k]}{\sum_{j \in \Gamma^{-1}(i)} \left[\overline{Q_{ij}}[k] + \sum_{\mu \in S_\mu^-} Q_{ij}^{\mu}[k] \right]} \tag{9}$$

where $\gamma_{ij}[k]$ represents the composite turning proportion from link i to link j at time interval k, and other parameters are same as in Section 2.1. In addition to the above network-wide approach with Equation (9), it is notable that the identification of turning fractions can also be made from local measurements of associated link or movement flows to overcome the fluctuation of traffic patterns among neighboring movements (Davis and Lan, 1995; Mirchandani et al., 2001). Therefore, the traffic control system can employ the following simple convex combination of the above two estimators to produce a more reliable estimation or projection of the turning proportions for real-world applications:

$$\gamma_{ij}[k] = \vartheta \cdot \gamma'_{ij}[k] + (1 - \vartheta) \cdot \gamma''_{ij}[k] \tag{10}$$

where ϑ is a weighting parameter between 0 and 1 that can be determined based on field calibrations; $\gamma'_{ij}[k]$ and $\gamma''_{ij}[k]$ are the projected turning proportions from Equation (9) and local measurement approaches, respectively.

It should be noted that reliable projection of turning proportions is also conditioned on how drivers respond to the diversion control under the given corridor network structure and traffic conditions. In real-world applications, one can employ real-time traffic measurements from the surveillance system to produce a reliable estimation of driver compliance rates in the current and previous control intervals, which will provide online feedback to the optimization model so as to adjust the set of diversion rates. The diversion compliance rate at off-ramp ν during the control interval h, denoted by $\widehat{\beta}_h^{\nu}$, can be easily updated by the following equation:

$$\widehat{\beta}_h^{\nu} = \left[\frac{\bar{q}_{\nu}^{in}[h]}{\bar{q}_{-1,N(i-1)}[h]} - \gamma_h^{\nu} \right] / z_h^{\nu} \tag{11}$$

where, $\bar{q}_{\nu}^{in}[h]$ and $\bar{q}_{-1,N(i-1)}[h]$ represent the online measurement of flow rates at the off-ramp ν and its upstream freeway mainline link during the control interval h, respectively; γ_h^{ν} is the normal exit rate for off-ramp ν during the control interval h; z_h^{ν} is the applied diversion rate during the control interval h. Note that the estimated driver compliance rates from Equation (11) are only for current and previous control intervals. However, one can still project compliance rates in the future time horizon by applying time series analysis approaches or by data mining of historical driver response patterns to the diversion control.

3 THE CONTROL MODEL AND SOLUTION

Based on the above extended corridor flow model, we develop a diversion control model that can yield the following outputs, including (1) a set of critical upstream off-ramps and downstream on-ramps to be used for detour operations (i.e., the control boundaries); (2) dynamic diversion rates and detour destinations for traffic at those critical upstream off-ramps within the incident impact boundaries; and (3) arterial signal timings including cycle lengths, offsets, and green splits over the entire control time period H. More specifically, we define the control decision vector to be $\mathbf{s} = (\mathbf{c}, \mathbf{g}, \mathbf{o}, \mathbf{w}, \mathbf{z})$ with $\mathbf{c} = (c_h | h \in H)$ (the common cycle length for all intersections in each control interval h), $\mathbf{g} = (g_h^{np} | n \in S_N, p \in P_n, h \in H)$ (the green time for phase p of intersection n for each control interval h), $\mathbf{o} = (o_h^n | n \in S_N, h \in H)$ (the offset of intersection n for each control interval h), $\mathbf{w} = (w_h^{\nu\mu} | \nu \in S_\nu^+, \mu \in S_\mu^-, h \in H)$ (the decision variable to divert traffic from upstream off-ramp ν to downstream on-ramp μ within the incident impact boundaries), and $\mathbf{z} = (z_h^\nu | \nu \in S_\nu^+, h \in H)$ (diversion rates at the incident upstream off-ramp ν for each control interval h).

3.1 Model formulation

The control model aims to maximize the utilization of available arterial capacity, and increase the total corridor throughput, given by

$$\max f_1(\mathbf{s}) = \sum_{t=1}^{H} q_{i+1,0}[t] \cdot \Delta T + \sum_{k=1}^{H} \sum_{i \in S^{OUT}} q_i^{in}[k] \tag{12}$$

where $q_{i+1,0}[t]$ represents the flow rate entering the downstream freeway link in the corridor network; S^{OUT} is the set of outgoing boundary links in the arterial system; therefore, $\sum_{k=1}^{H} \sum_{i \in S^{OUT}} q_i^{in}[k]$ denotes the total number of vehicles entering the boundary links in the arterial.

Another objective function of the control model is designed to reflect the perspective of detour travelers, which aims at minimizing their total time spent on the detour route so as to ensure their compliance to the routing guidance, given by

$$\min f_2(\mathbf{s}) = \sum_{k=1}^{H} \left[\sum_{i \in S^U} \sum_{\mu \in S_\mu^-} N_i^\mu[k] + \sum_{\nu \in S_\nu^+} \sum_{i \in S_\mu^-} N_\nu^\mu[k] + \sum_{\mu \in S_\mu^-} N_\mu^\mu[k] \right] \cdot \Delta t \tag{13}$$

where $N_i^\mu[k]$, $N_\nu^\mu[k]$, and $N_\mu^\mu[k]$ represent the number of detour vehicles heading to on-ramp μ that are traveling at link i, off-ramp ν, and on-ramp μ within the incident impact boundaries at time step k, respectively; S^U is the set of arterial links; S_ν^+ is the set of off-ramps upstream of the incident location; and S_μ^- represents the set of on-ramps downstream of the incident location.

In summary, the biobjective mathematical expression of the proposed generalized corridor control model is given below:

$$\min f(\mathbf{s}) = [-f_1(\mathbf{s}), f_2(\mathbf{s})]^T \tag{14}$$

Subject to:

$$\forall \mathbf{s} \in \Omega = \{\mathbf{s} | c_{min} \le c_h \le c_{max} \forall h \in H \tag{15}$$

$$g_{min}^{np} \le g_h^{np} < c_h \quad \forall n \in S_N, p \in P_n, h \in H \tag{16}$$

$$c_h = \sum_{p \in P_n} g_h^{np} + \sum_{p \in P_n} I^{np} \quad \forall n \in S_N, p \in P_n, h \in H \tag{17}$$

$$0 \le o_h^n \le c_h \quad \forall n \in S_N, h \in H \tag{18}$$

$$\sum_{\mu \in S_\mu^-} w_h^{\nu\mu} \le 1 \quad \forall \nu \in S_\nu^+, h \in H \tag{19}$$

$$\beta_h^\nu \cdot z_h^\nu + \gamma_h^\nu \le z_{max} \quad \forall \nu \in S_\nu^+, h \in H \} \tag{20}$$

where Ω is the feasible solution set; S_N is the set of arterial intersections; c_{min} and c_{max} are the minimum and maximum cycle lengths; P_n is the set of signal phases at intersection n; g_{min}^{np} is the minimal green time for phase p of intersection n; and I^{np} is the intergreen time for phase p of intersection n. z_{max} is the maximum percentage of traffic (including both detour and normal exiting) that can diverge from freeway to arterial.

Equation (15) restricts the common cycle length to be between the minimal and maximal values. Equation (16) requires that the green time for each phase should at least satisfy the minimal green time and no more than the cycle length. The sum of green times and intergreens for all phases at intersection n should be equal to the cycle length by Equation (17). Moreover, the offset of intersection n is constrained by Equation (18) to be between 0 and the cycle length. Equation (19) ensures that traffic at any upstream off-ramp can be detoured to no more than one downstream on-ramp during the same control interval h; and the diversion rate is bounded by Equation (20) with β_h^ν and γ_h^ν representing the driver compliance rate and the normal off-ramp exiting rate.

3.2 Solution algorithm

GA-based heuristics have been successfully demonstrated to yield viable and metaoptimal solutions to a

series of combinatorial optimization problems in a reasonable time period (Kim and Adeli, 2001; Teklu et al., 2007; Al-Bazi and Dawood, 2010; Marano et al., 2011; Hsiao et al., 2012; Sgambi et al., 2012). This study has employed the GA integrated with the rolling time horizon approach to solve the proposed model. Other heuristics can certainly be adopted to solve the proposed model as long as they satisfy the computational time requirement for online application. The two objectives in the control model are first normalized into the same scales, and then weighted to a single function for optimization, given by

$$r(\mathbf{s}) = \sqrt{\varepsilon_1 \cdot \left(\frac{f_1(\mathbf{s}) - f_1^{\min}(P)}{f_1^{\max}(P) - f_1^{\min}(P)}\right)^2 + \varepsilon_2 \cdot \left(\frac{f_2(\mathbf{s}) - f_2^{\min}(P)}{f_2^{\max}(P) - f_2^{\min}(P)}\right)^2}, \quad \mathbf{s} \in P \tag{21}$$

where P represents the current population of GA; $\varepsilon_m | m = 1, 2$ is the weight assigned to objective function m to emphasize its degree of importance. $f_m^{\min}(P) = \min\{f_m(\mathbf{s}) | \mathbf{s} \in P\}$ and $f_m^{\max}(P) = \max\{f_m(\mathbf{s}) | \mathbf{s} \in P\}$ represent the minimum and the maximum values of the objective function at the current population P, respectively. Note that the smaller the $r(\mathbf{s})$ is, the better the individual will be in the current GA population. To generate feasible control parameters that satisfy the operational constraints, one needs to develop the following decoding scheme.

A total number of NP_n fractions $(\lambda_h^p | p = 1 \cdots NP_n)$ are generated for the controller at intersection n during each control interval h from decomposed binary strings, where NP_n is the number of phases of intersection n. These fractions are used to code the green times and offsets as follows:

$$g_h^{np} = g_{\min}^{np} + \left(c_h - \sum_{p \in P_n} g_{\min}^{np} - \sum_{p \in P_n} I^{np}\right) \cdot \lambda_h^p \times \prod_{j=1}^{p} \left(1 - \lambda_h^{j-1}\right) \tag{22}$$
$$p = 1 \cdots NP_n - 1, \quad n \in S_N, h \in H$$

$$g_h^{np} = g_{\min}^{np} + \left(c_h - \sum_{p \in P_n} g_{\min}^{np} - \sum_{p \in P_n} I^{np}\right) \times \prod_{j=1}^{p} \left(1 - \lambda_h^{j-1}\right), \quad p = NP_n, n \in S_N, h \in H \tag{23}$$

$$o_h^n = (c_h - 1) \cdot \lambda_h^{NP}, n \in S_N, h \in H \tag{24}$$

And the cycle length at intersection n during control interval h can be decoded from an additional random real number fraction λ_h^c transformed from the decomposed binary string, given by

$$c_h = c_{\min} + (c_{\max} - c_{\min}) \cdot \lambda_h^c \tag{25}$$

To properly relate the control decision variables with the signal state variables in the corridor flow model, the following mapping functions are developed:

$$(\delta_1^{np}[k] - 0.5) \cdot \mathrm{mod}(k - o_h^n, c_h) \le (\delta_1^{np}[k] - 0.5) \times \sum_{j=1}^{p-1} (g_h^{nj} + I^{nj}) \tag{26}$$

$$(\delta_2^{np}[k] - 0.5) \cdot \mathrm{mod}(k - o_h^n, c_h) > (\delta_2^{np}[k] - 0.5) \times \left[\sum_{j=1}^{p-1} (g_h^{nj} + I^{nj}) + g_h^{np}\right] \tag{27}$$

$$\delta_1^{np}[k] + \delta_2^{np}[k] + g^{np}[k] = 1 \tag{28}$$

where $g^{np}[k]$ is a binary value indicating whether signal phase p of intersection n is set to green at time step k in the arterial flow model; $\delta_1^{np}[k]$ and $\delta_2^{np}[k]$ are two sets of auxiliary 0–1 variables to obtain the status of $g^{np}[k]$.

To generate diversion rates constrained by (20), the following relation function is used to transform the random real number fraction λ_h^v that is generated from the decomposed binary string:

$$z_h^v = \frac{z_{\max} - \gamma_h^v}{\beta_h^v} \cdot \lambda_h^v, \quad \forall v \in S_v^+, h \in H \tag{29}$$

To satisfy (19), this study randomizes an integer vector $(l_h^v | v \in S_v^+, h \in H)$, where l_h^v is the index of incident downstream on-ramp to which traffic from upstream off-ramp v is detoured during control interval h. Then, we have

$$w_h^{vl_h^v} = 1, \quad \text{if } l_h^v \neq 0; w_h^{vl_h^v} = 0, \quad \text{if } l_h^v = 0$$

By employing the aforementioned decoding schemes, the solution vector during GA evolution is always assured to be feasible. The step-by-step description of the GA searching routine is not the focus of this article and will not be detailed in this section.

This study has further integrated the GA with the rolling time horizon approach, which has been commonly used to optimize the control plans in real-time applications, based on the projection of traffic conditions within each stage. The optimized control plan is only implemented within the first control interval of

that stage. Then, the optimization process starts all over again with feedback from the real-time surveillance system, and the control horizon shifts forward by one control interval. In real-world applications, lengths of the projection stage and the control update interval need to be carefully set to perform a trade-off between the computing efficiency and the model accuracy.

4 CASE STUDY

4.1 The corridor network

To illustrate the applicability of the generalized corridor model, this study has employed a stretch of I-94 East–West corridor between downtown Milwaukee and Waukesha for case study. This 12-mile corridor stretch includes 12 freeway ramps and 29 signalized intersections along the alternative route (US-18). Layout of the corridor network is given in Figure 3. I-94 mainline westbound has three lanes, and US-18 is a major arterial with two lanes in each direction.

4.2 Calibration of the corridor flow model

This study consists of utilizing multiple data sources to calibrate the corridor flow model, including stated preferences of drivers, volume counts, and speeds at multiple screen lines and intersections, surveillance and field recorded videos, and vehicle tracking with Bluetooth detection. The volume counts and speeds were used to calibrate the speed–density function parameters and flow propagation and conservation equations. The video surveillance on the freeway help to determine the merging- and diverging-related model parameters, and the videos on the alternate route produce traffic counts at intersections and arterial streets for the lane-group model calibration. With Bluetooth detection, one can track a vehicle along different segments of the freeway, which helps to provide valuable average speed and travel time information to fine-tune the calibrated model parameters. The traveler survey results reveal the behaviors of travelers in response to the incident and give insights on the real-world application of the proposed model.

Traffic data from Wavetronix units, TRAffic Database System (TRADAS), Automatic Traffic Recorder (ATR) stations, and tube counters were archived in the Volume, Speed, and Occupancy Application Suite (V-SPOC) of the WisTransportal Data Hub maintained by UW-Madison and Wisconsin Department of Transportation, which makes them easily accessible to traffic engineers and researchers. One can download the aggregated sensor data, which is in CSV format, for any date and time interval dating back to 1996. Real-time Bluetooth devices were used in the data collection and the data were downloaded directly in CSV format in any 15-minute time increments. A total of 13 Bluetooth stations were deployed in data collection and all of them were placed at approximately the same locations as V-SPOC sensor stations to correlate traffic volume and travel time information. Solar panels were used to charge the batteries of the Bluetooth devices so that they could be used for the entire study period. In all of the studies, there were no reported power failures resulting in time intervals with no data. The dates for data collection were set between May 6, 2012 and May 23, 2012. For the purpose of simplicity, we have ignored the vehicle classification in the data set. During the data collection period, an accident occurred on the I-94 mainline westbound between ramps 5 and 6 at around 4:45 PM on May 9, 2012. The accident lasted about 40 minutes and blocked one lane in the westbound direction.

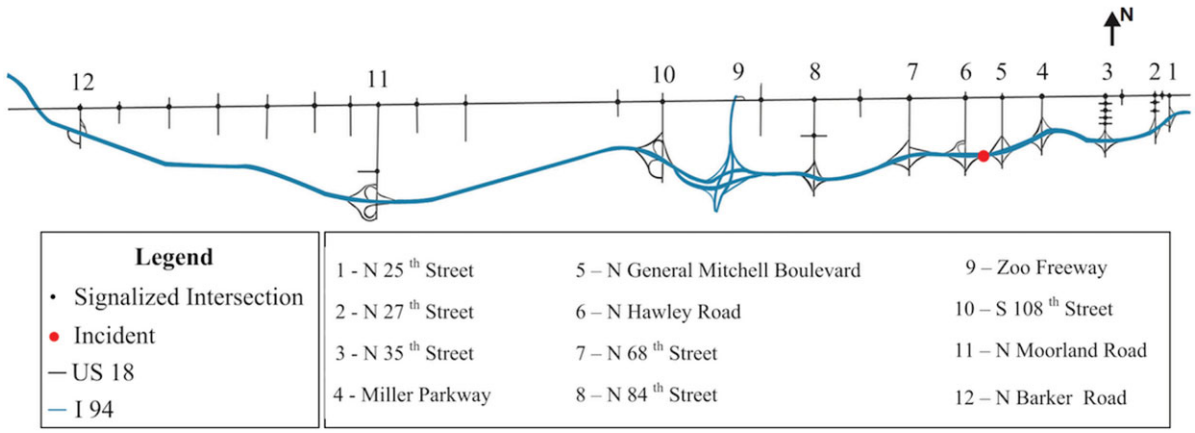

Fig. 3. The study corridor network.

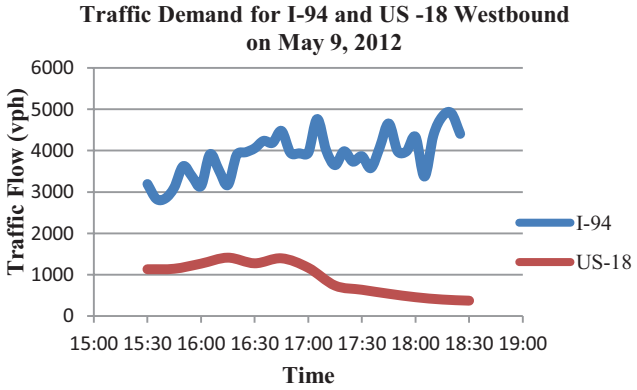

Fig. 4. Traffic volume for I-94 and US-18 westbound on May 9, 2012 for case study.

In this study, evening peak period's data (3:30–6:30 PM) on May 9 was used to calibrate and evaluate the proposed model with a sampling interval of 5 minutes (see Figure 4 for westbound traffic volume distribution). Transferability of the calibrated model parameters to other days will also be evaluated.

Let $\theta = (v_{min}, \rho_{jam}, \rho_{min}, \rho_{cr}, \alpha, \beta, \alpha_f, \phi, \varphi, \eta, \tau, \kappa)$ be the model parameter vector. The calibration process aims to minimize the quadratic errors between the model-estimated and measured values of speeds and volumes for all sections in the corridor with data available, given by

$$\min \mathcal{F}(\theta) = \frac{\Delta s}{n_U H} \sum_{i \in S^U} \sum_{j \in \Gamma^{-1}(i)} \sum_{k=1}^{H/\Delta s} \Big[\varpi_q (Q_{ij}[k] - Q'_{ij}[k])^2 \Big] + \frac{\Delta s}{n_F H} \sum_{i \in S^F} \sum_{t=1}^{H/\Delta s} \big[(v_i[t] - v'_i[t])^2 + \varpi_q (q_i[t] - q'_i[t])^2 \big] \quad (30)$$

where Δs is the length of the sampling interval; n_U is the number of links in the arterial; n_F is the number of freeway and ramp sections; ϖ_q is the weight applied to volumes for them to be comparable with speeds; $Q'_{ij}[k]$, $v'_i[t]$, and $q'_i[t]$ are the measured values of volumes and speeds. Due to the missing data problems, speeds are not always available at all freeway sections in certain sampling intervals. In that case, only volumes are used for calibration. To obtain a reasonable balance between speed and volume errors, ϖ_q was set at 0.00028 considering the volume and speed level in the I-94 corridor.

The calibration model is nonlinear, therefore may end with local minima. We further use travel times measured from a total of 2,322 Bluetooth pairs and 987 triples to fine-tune the parameter based on the following fitness evaluation function:

$$r(TT) = 1 - \frac{E[(TT - TT')^2]}{E[TT'^2]} \quad (31)$$

Table 1
Calibrated corridor flow model parameters used in the case study

Parameters	*Values*
$\Delta t, \Delta T$ (seconds)	1.0, 5.0
ρ_{jam}, $\rho_{\min}$, ρ_{cr} (veh/mile/lane)	210, 20.6, 53.9
$v_{\min}$ (mph)	0.0
α, β	2.96, 1.87
α_f	1.746
ϕ	1.683
φ	0.987
η (mile^2/h)	4.98
τ (seconds)	27
κ (veh/mile/lane)	19.8
Freeway segment length (feet)	800
Discharge capacity (vphpl)	Freeway mainline (2,200), arterial (1,800), ramps (1,900)
Average vehicle length (feet)	24.0
Free flow speed (mph)	Freeway mainline (62.3), arterial (34.9), ramps (31.6)

The calibration process was implemented in C++ on a work station with an Intel Core i7-3770S Ivy Bridge 3.9 GHz Turbo CPU and 32 GB RAM. The 12-mile I-94 freeway mainline westbound stretch was divided into 80 sections and a total of 96 movements at eight arterial intersections were used for calibration. The calibration process runs for 5.32 hours and the parameter set after optimization is shown in Table 1 with the $r(TT) = 0.891$, which indicates acceptable consistency between the corridor model and the measured data.

The fitted model parameter set also shows to be fairly transferable over data on other days between May 6, 2012 and May 23, 2012 with $r(TT)$ ranging from 0.831 to 0.878.

4.3 Experimental analysis and results

With the calibrated corridor flow model, this section evaluates the control model's performance under the incident scenario on May 9, 2012. The entire evaluation period is 3 hours of peak period from 3:30 to 6:30 PM, including the first interval of 75 minutes (3:30–4:45 PM) for normal operation, the second interval of 40 minutes (4:45–5:25 PM) with incident, and the final interval of 65 minutes (5:25–6:30 PM) for recovery. A 100% driver compliance rate is assumed for model evaluation. Key

Table 2
Key control model and algorithm parameters used in the case study

c_{min}, c_{max} (seconds)	60, 160
g_{min}^{np}, I^{np} (seconds)	7, 4
z_{max}	0.50
GA population size	100
Maximum number of generations	200
Crossover probability	0.6
Mutation probability	0.02
Length of projection stage in rolling time horizon (minutes)	10
Length of control interval (minutes)	$2c_h$

parameters used in the control model are summarized in Table 2.

This section will evaluate the performance of the proposed generalized diversion model with the following steps:

- Investigate the impacts of different weight assignment settings on the control area (critical off-ramps and on-ramps involved) generated from the proposed model and the system measure of effectiveness (MOEs).
- Compare the performance of the proposed model with the single-segment diversion model proposed by Liu et al. (2011).
- Perform sensitivity analysis of the proposed model to different levels of driver compliance rates by comparing its performance with the integrated diversion control model by Wu and Chang (1999).

4.3.1 The impact of different assigned weights on the control boundaries and system MOEs. Table 3 presents the variation of the control boundaries generated from the proposed model with the assigned weights of $\varepsilon_1/\varepsilon_2$ ranging from 10/0 to 0/10 for the study corridor network, and Table 4 summarizes its impact on the system MOEs. Comparison between the results yields the following findings:

- With the weight assignment between two control objectives varying from 10/0 to 0/10, the generated control area shrinks and the total diversion rate decreases as expected.
- Depending on the traffic conditions and corridor network structure, there exists a critical control area beyond which the total corridor throughput no longer increases. For example, while the study network covers a 12-ramp stretch, only four upstream off-ramps and two downstream on-ramps are used to yield the maximal corridor throughput and minimal total travel time (see Table 3).
- The number of incident downstream on-ramps used to divert traffic back to the freeway is less than that of incident upstream off-ramps, which makes sense since the higher capacity at incident-free freeway links may encourage detour traffic to come back to the freeway whenever it is available.
- Compared with the control boundaries generated by maximizing the total corridor throughput only (i.e., $\varepsilon_1/\varepsilon_2 = 10/0$), the one obtained by setting $\varepsilon_1/\varepsilon_2 = 7/3$ seems more appropriate for the test corridor network due to its compact size and shorter distances for detour operations, which can significantly save the traffic management resources. Most importantly, it can substantially reduce the required total diversion rates as well as the total time spent by the detour traffic (15.1% and 23.3%, respectively, as shown in Table 4) at the relatively low reduction in the total corridor throughput (3.9%) and slight increase of total corridor travel time (4.7%). In real-world applications, traffic operators can refer to the same procedure to determine the proper control boundaries, and achieve the maximal control benefits under the given incident scenario.

This study has also explored the distribution of diversion flows over different off-ramps and on-ramps within the control area under various weights between two control objectives. The comparison results, as shown in Table 5, have indicated that

- The diversion flows are not evenly distributed over the ramps. An off-ramp closer to the incident location has carried most diversion flows, and the on-ramp closer to the incident location has also received more detoured flows. This is reasonable as traffic prefers to reduce the extra travel distances caused by the detour operations, and comes back to the freeway as soon as possible to best use the high capacity at incident-downstream freeway links.
- Traffic operators shall set weights to obtain a proper control area without those marginal ramps (e.g., off-ramps at 2 and 3 with low diversion volumes), as they incur excessive detour times, but do not substantially contribute to the improvement of corridor system performance. Such findings again verify the previous argument of obtaining an appropriate control area by setting $\varepsilon_1/\varepsilon_2 = 7/3$ (significant savings in total diversion time with trivial reduction in total corridor throughput and slight increase in total corridor travel time).

Figure 5 illustrates the time-varying detour travel time over freeway travel time ratios. One can observe

Table 3
The control boundaries generated from the model under different weight assignment

	Control boundaries (Ramp IDs)											
	Incident upstream					*Incident downstream*						
$\varepsilon_1/\varepsilon_2$	*Ramp 1*	*Ramp 2*	*Ramp 3*	*Ramp 4*	*Ramp 5*	*Ramp 6*	*Ramp 7*	*Ramp 8*	*Ramp 9*	*Ramp 10*	*Ramp 11*	*Ramp 12*
10/0		X	X	X	X	X	X					
9/1		X	X	X	X	X	X					
8/2			X	X	X	X	X					
7/3				X	X	X	X					
6/4				X	X	X	X					
5/5				X	X	X						
4/6				X	X	X						
3/7				X	X	X						
2/8					X	X						
1/9					X	X						
0/10												

Note: Ramp ID with an "X" represents that incident upstream off-ramp or downstream on-ramp at the target ramp is included in the control boundaries.

Table 4
System MOEs under various weight assignment

	Corridor MOEs			
$\varepsilon_1/\varepsilon_2$	*Total corridor throughput (vehs)*	*Total corridor travel time (veh-hours)*	*Total diversion volume (vph)*	*Total time spent by detour traffic (veh-hours)*
10/0	14,057	6,091.37	1,860	1,336.61
9/1	13,826	6,202.85	1,803	1,333.31
8/2	13,604	6,325.09	1,769	1,145.60
7/3	13,511 (−3.9%)	6,377.74 (+4.7%)	1,579 (−15.1%)	1,025.19 (−23.3%)
6/4	12,904	6,752.32	1,382	916.81
5/5	11,889	7,428.89	1,078	638.06
4/6	11,591	7,632.35	945	537.12
3/7	11,298	7,837.84	800	432.68
2/8	10,778	8,219.18	542	295.39
1/9	10,383	8,514.83	388	149.09
0/10	9,335	9,405.97	0	0.00

that by setting the weight assignment as $\varepsilon_1/\varepsilon_2 = 7/3$, the assumed 100% of driver compliance rates could be achieved since the detour travel time is less than or comparable to the freeway travel time during the incident occurring and recovery periods (i.e., control intervals 15–32). Such a finding also indicates that the weight assignment must be set at a critical value to ensure that the ratio of detour travel time to freeway travel time is less than or around 1.0 to ensure acceptable driver compliance levels. Figure 6 shows the time evolution of diversion flows at ramps 4 and 5 when setting $\varepsilon_1/\varepsilon_2 = 7/3$.

4.3.2 Comparison between the extended model and alternative control strategies. In this analysis, the performance of the proposed model will be compared with an alternative control strategy to validate its effectiveness in incident management. The study network shown in Figure 3 with the same experimental design is employed for comparison with CORSIM as the unbiased evaluator:

- Alternative I: The integrated control model proposed by Liu et al. (2011) with only one segment between ramps 5 and 6 under control, and the control objective is to maximize the total corridor throughput.
- Alternative II: The proposed diversion control model with $\varepsilon_1/\varepsilon_2 = 7/3$.

Table 6 summarizes the comparison results between the both models with respect to the following five types

Table 5
Distribution of diversion flows (in vph) at incident upstream and downstream ramps

		Weights assignment $\varepsilon_1/\varepsilon_2$									
	Ramps	*10/0*	*9/1*	*8/2*	*7/3*	*6/4*	*5/5*	*4/6*	*3/7*	*2/8*	*1/9*
1		–	–	–	–	–	–	–	–	–	–
2	Incident	161	101	–	–	–	–	–	–	–	–
3	Upstream	254	249	146	–	–	–	–	–	–	–
4	Off-ramps	681	643	725	667	445	279	173	51	–	–
5		765	810	898	912	937	799	772	749	542	388
6		834	815	869	827	891	954	874	757	521	376
7		630	610	610	487	317	–	–	–	–	–
8	Incident	–	–	–	–	–	–	–	–	–	–
9	Downstream	–	–	–	–	–	–	–	–	–	–
10	On-ramps	–	–	–	–	–	–	–	–	–	–
11		–	–	–	–	–	–	–	–	–	–
12		–	–	–	–	–	–	–	–	–	–

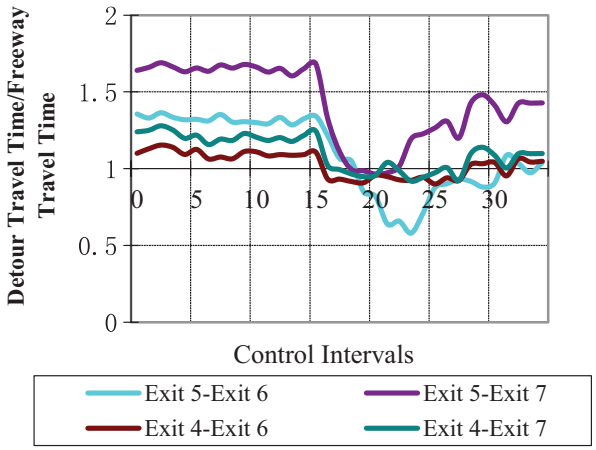

Fig. 5. Time-varying detour travel time over freeway travel time ratio ($\varepsilon_1/\varepsilon_2 = 7/3$).

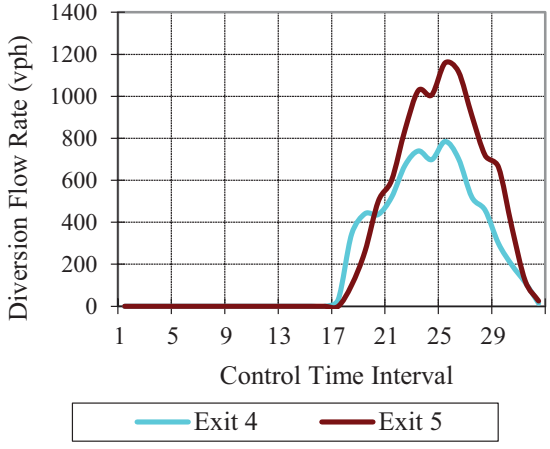

Fig. 6. Time-varying diversion rates at off-ramps ($\varepsilon_1/\varepsilon_2 = 7/3$).

of performance indices: (1) total diversion rate; (2) total corridor throughput; (3) total corridor travel time; (4) average detour route delay time; and (5) total side street queue time.

Comparison between the results in Table 6 yields the following findings:

- The proposed model outperforms the single-segment diversion model in terms of the total corridor throughput and total corridor travel time (19.1% and 23.3%) due to the fact that using only one corridor segment is subject to the limitation of flow capacity at the ramp or the intersection turning lane. However, with multiple ramps for integrated diversion control, one can overcome such limitation by balancing the detour traffic load over multiple ramps and intersection turning lanes, which results in a higher rate of diversion flows (1,579 versus 1,095) and better utilized network capacity.
- The advantage of the proposed model is also indicated by the significant decrease in average detour route delay time (−33.6%) and total side street queue time (−41.9%). Compared with the single-segment diversion model, this result is desirable as it encourages traffic to follow the detour operations and avoids the excessive delays to the side street traffic.

4.3.3 Sensitivity of model performance to driver compliance. The promising performance of the proposed model is conditioned on a 100% level of diversion compliance rates. However, during real-world operations, driver behavioral patterns are usually subject to time-varying fluctuations. To address the above critical

Table 6
Comparison results between the proposed model and the single-segment diversion model

Performance indices	*The single-segment diversion model*	*The proposed model*	*Improvement*
Total diversion rates (vph)	1,095	1,579	+44.2%
Total corridor throughput (vehs)	11,345	13,511	+19.1%
Total corridor travel time (veh-hours)	8,313.45	6,377.74	−23.3%
Average detour route delay time (minutes)	16.38	10.87	−33.6%
Total side street queue time (veh-hours)	43.31	25.15	−41.9%

Table 7
Sensitivity analysis with respect to the variation of diversion compliance rates

	System MOEs			
Diversion compliance rates	*Total travel time savings (veh-hours)*	*Improvement (%)*	*Total throughput increases (vehs)*	*Improvement (%)*
100%	308.45	5.29%	949	7.35%
95%	271.33	5.07%	873	7.02%
85%	221.67	4.91%	731	9.92%
70%	195.32	4.98%	698	10.31%
50%	112.08	5.23%	540	9.42%
35%	91.73	4.01%	339	8.73%

Note: The total time savings and total throughput increases are obtained based on the comparison with the integrated diversion model by Wu and Chang (1999).

issue, this section has evaluated the performance of the proposed control model under the designed experimental scenarios, with the diversion compliance rates at the 95%, 85%, 70%, 50%, and 35% levels, respectively. The control objective is set to maximize the total corridor throughput. Table 7 has summarized the sensitivity of proposed model performance to diversion compliance rates in comparison with the model by Wu and Chang (1999).

As illustrated in Table 7, the performance of the proposed control model declines with the decrease of the diversion compliance rates. For example, the savings of total travel time drop from 308.45 to 91.73 veh-hours with the decrease of diversion compliance level from 100% to 35%, and the increases of total corridor throughput decline from 949 to 339 vehs similarly. However, the improvement of the model performance over the integrated diversion model by Wu and Chang (1999) seems not to be sensitive to the decrease of the diversion compliance rates, which has indicated the potential for an application of the proposed model in the traffic environment with significant discrepancy in driver behavioral patterns.

5 CONCLUSION

This study has presented a generalized diversion control model for freeway incident management that is capable of concurrently optimizing the detour rates and arterial signal timings over multiple roadway segments between the freeway and its neighboring arterial. To capture various operational complexities due to the interactions between multiple diversions, this study has extended the model developed in our previous work and integrated it in the overall corridor optimization process. Case studies using a stretch of I-94 corridor network have confirmed the conclusions that:

- The generalized corridor model offers the flexibility for traffic operators to determine the proper time and control points to implement diversion control, which can help to prioritize the limited control resources and achieve the best operational efficiency.
- Compared with the single-segment diversion model by Liu et al. (2011), the generalized corridor model can substantially improve the utilization of corridor capacity by balancing the detour traffic load over multiple ramps and intersection turning lanes, which can effectively prevent the excessive delays on the detour route.
- The proposed diversion model is sufficiently reliable for use under the traffic environment with significant discrepancy in driver behavioral patterns and outperforms another advanced integrated diversion control strategy by Wu and Chang (1999).

Despite the effectiveness of this study in overcoming several critical issues for the real-time corridor diversion control under incident conditions, a more efficient and reliable solution for implementing such a system in network-wide applications remains essential. Further studies along this line include:

1. Development of efficient solution algorithms for integrated network-wide control

This study has employed a GA-based heuristic to solve the corridor diversion control formulations. For a large-scale network-wide application, the chromosome length will increase, and the GA-based heuristic will need a larger size of population and/or more generations of evolution to converge to a reliable solution, which may limit its efficiency in real-time applications. One potential solution to tackle this critical issue is to intelligently decompose the large corridor network into a series of subnetworks such that the search directions of the problem can be significantly narrowed down, and the parallel computing technique can also be employed for more efficient multitasking system operations and communications. Alternately, one may investigate other heuristics that are less sensitive to the dimensionality of the solution space size. For example, by employing the Simultaneous Perturbation Stochastic Approximation (SPSA) approach, it may yield the efficient solution for large-scale corridor networks. However, depending on the corridor network structure and traffic conditions, some key searching parameters of the SPSA need to be calibrated in advance to ensure its performance.

2. Development of robust solution algorithms for the proposed model when available control inputs are missing or contain some errors

The performance of the proposed corridor diversion control model is conditioned on the quality and availability of input data from the surveillance system. However, the availability and accuracy of the existing surveillance system always suffer from the hardware quality deficiency. Neglecting the impact of the data quality in the model formulations may degrade both operational efficiency and reliability in real-world applications. To contend with such deficiencies embedded in the existing models, one needs to develop a robust algorithm to account for measurement errors in system inputs so that it can yield control strategies less sensitive to the data measurement errors.

3. Development of an intelligent interface with advanced surveillance systems

For real-time implementation of the proposed control model, it requires real-time realization of the control input data from various sources of the surveillance system. This article has presented an online estimation approach for control parameters used in the proposed control system in Section 2.3. Many advanced detection technologies developed in recent years in the traffic control field have featured their capabilities in capturing the evolution of traffic flows at each individual movement or vehicle level, which offers the promise for a real-time control system to significantly reduce the cost in data processing and parameter estimation. Hence, to effectively operate an integrated real-time corridor control system, one should certainly develop an intelligent interface to take advantage of those features embedded in the emerging advanced detection technologies.

ACKNOWLEDGMENTS

This research is supported by the University of Wisconsin-Milwaukee Research Growth Initiative Program, the National Natural Science Foundation of China under Grant No. 51108248, and the National Natural Science Foundation of Shandong under Grant No. ZR2011GQ002.

REFERENCES

Adeli, H. & Ghosh-Dastidar, S. (2004), Mesoscopic-wavelet freeway work zone flow and congestion feature extraction model, *Journal of Transportation Engineering*, **130**(1), 94–103.

Adeli, H. & Jiang, X. (2009), *Intelligent Infrastructure Neural Networks, Wavelets, and Chaos Theory for Intelligent Transportation Systems and Smart Structures*, CRC Press, Taylor & Francis, Boca Raton, FL.

Adeli, H. & Karim, A. (2005), *Wavelets in Intelligent Transportation Systems*, John Wiley and Sons, West Sussex, United Kingdom.

Al-Bazi, A. & Dawood, N. (2010), Developing crew allocation system for precast industry using genetic algorithms, *Computer-Aided Civil and Infrastructure Engineering*, **25**(8), 581–95.

Ben-Akiva, M., Bottom, J. & Ramming, M. S. (2001), Route guidance and information systems. *Journal of Systems and Control Engineering*, **215**(4), 317–24.

Bhaskar, A., Chung, E. & Dumont, A. G. (2011), Fusing loop detector and probe vehicle data to estimate travel time statistics on signalized urban networks, *Computer-Aided Civil and Infrastructure Engineering*, **26**(6), 433–50.

Chang, G. L., Ho, P. K. & Wei, C. H. (1993), A dynamic system-optimum control model for commuting traffic corridors, *Transportation Research*, **1C**, 3–22.

Cremer, M. & Schoof, S. (1989), On control strategies for urban traffic corridors, in *Proceedings of IFAC Control, Computers*, Communications in Transportation, Paris.

Davis, G. A. & Lan, C. J. (1995), Estimating intersection turning movement proportions from less-than-complete sets of traffic counts, *Transportation Research Record*, **1510**, 53–59.

Duthie, J. C., Unnikrishnan, A. & Waller, S. T. (2011), Influence of demand uncertainty and correlations on traffic predictions and decisions, *Computer-Aided Civil and Infrastructure Engineering*, **26**(1), 16–29.

Hooshdar, S. & Adeli, H. (2004), Toward intelligent variable message signs in freeway work zones: a neural network approach, *Journal of Transportation Engineering*, **130**(1), 83–93.

Hsiao, F. Y., Wang, S. S., Wang, W. C., Wen, C. P. & Yu, W. D. (2012), Neuro-fuzzy cost estimation model enhanced by fast messy genetic algorithms for semiconductor hookup construction, *Computer-Aided Civil and Infrastructure Engineering*, **27**(10), 764–81.

Iftar, A. (1995), A decentralized routing controller for congested highways, in *Proceedings of 34th Conference on Decision and Control*, New Orleans, LA, 4089–94.

Jiang, X. & Adeli, H. (2003), Freeway work zone traffic delay and cost optimization model, *Journal of Transportation Engineering*, **129**(3), 230–41.

Kaparias, I., Bell, M., Chen, Y. & Bogenberger, K. (2007), IC-NavS: a tool for reliable dynamic route guidance, *IET Intelligent Transportation Systems* **1**(4), 225–53.

Karim, A. & Adeli, H. (2002), Incident detection algorithm using wavelet energy representation of traffic patterns, *Journal of Transportation Engineering*, **128**(3), 232–42.

Karim, A. & Adeli, H. (2003), Fast automatic incident detection on urban and rural freeways using wavelet energy algorithm, *Journal of Transportation Engineering*, **129**(1), 57–68.

Karoonsoontawong, A. & Lin, D. Y. (2011), Time-varying lane-based capacity reversibility for traffic management, *Computer-Aided Civil and Infrastructure Engineering*, **26**(8), 632–46.

Kim, H. & Adeli, H. (2001), Discrete cost optimization of composite floors using a floating point genetic algorithm, *Engineering Optimization*, **33**(4), 485–501.

Kotsialos, A., Papageorgiou, M., Mangeas, M. & Haj-salem, H. (2002), Coordinated and integrated control of motorway networks via non-linear optimal control, *Transportation Research*, **10C**, 65–84.

Lafortune, S., Sengupta, R., Kaufman, D. E. & Smith, R. L. (1993), Dynamic system-optimal traffic assignment using a state space model, *Transportation Research*, **27B**, 451–73.

Liu, Y. & Chang, G. L. (2011), An arterial signal optimization model for intersections experiencing queue spillback and lane blockage, *Transportation Research Part C*, **19**(1), 130–44.

Liu, Y., Chang, G. L. & Yu, J. (2011), An integrated control model for freeway corridor under non-recurrent congestion, *IEEE Transactions on Vehicular Technology*, **60**(4), 1404–18.

Liu, Y., Yu, J., Chang, G. L. & Rahwanji, S. (2008), A lane-group based macroscopic model for signalized intersections account for shared lanes and blockages, in *Proceedings of IEEE Conference on Intelligent Transportation Systems, ITSC*, 639–44.

Mahmassani, H. S. & Peeta, S. (1993), Network performance under system optimal and user equilibrium dynamic assignments: implications for advanced traveler information systems, *Transportation Research Record*, **1408**, 83–93.

Mammar, S., Messmer, A., Jensen, P., Papageorgiou, M., Haj-Salem, H. & Jensen, L. (1996), Automatic control of variable message signs in Aalborg, *Transportation Research*, **4C**, 131–50.

Marano, G. C., Quaranta, G. & Monti, G. (2011), Modified genetic algorithm for the dynamic identification of structural systems using incomplete measurements, *Computer-Aided Civil and Infrastructure Engineering*, **26**(2), 92–110.

Messmer, A. & Papageorgiou, M. (1990), METANET: a macroscopic simulation program for motorway networks, *Traffic Engineering and Control*, **31**, 466–70.

Messmer, A. & Papageorgiou, M. (1994), Automatic control methods applied to freeway network traffic, *Automatica*, **30**, 691–702.

Messmer, A. & Papageorgiou, M. (1995), Route diversion control in motorway networks via nonlinear optimization, *IEEE Transaction on Control System Technology*, **3**, 144–54.

Messmer, A., Papageorgiou, M. & Mackenzie, N. (1998), Automatic control of variable message signs in the interurban Scottish highway network, *Transportation Research C*, **6**, 173–87.

Mirchandani, P. B., Nobe, S. A. & Wu, W. (2001), Online turning proportion estimation in real-time traffic-adaptive signal control, *Transportation Research Record*, **1748**, 80–86.

Moreno-Banos, J. C., Papageorgiou, M. & Schäffner, C. (1993), Integrated optimal flow control in traffic networks, *European Journal of Operations Research*, **71**, 317–23.

Muñoz, J. C. & Laval, J. A. (2006), System optimum dynamic traffic assignment graphical solution method for a congested freeway and one destination, *Transportation Research Part B*, **40**(1), 1–15.

Nie, Y. & Wu, X. (2010), Providing reliable route guidance: a case study using Chicago data, in *Proceedings of the 89th Transportation Research Board Annual Meeting*, Washington DC.

Nsour, S. A., Cohen, S. L., Clark, J. E. & Santiago, A. J. (1992), Investigation of the impacts of ramp metering on traffic flow with and without diversion. *Transportation Research Record*, **1365**, 116–24.

Papageorgiou, M. (1990), Dynamic modeling, assignment, and route guidance in traffic networks, *Transportation Research*, **24B**, 471–95.

Papageorgiou, M. (1995), An integrated control approach for traffic corridors, *Transportation Research*, **3C**, 19–30.

Pavlis, Y. & Papageorgiou, M. (1999), Simple decentralized feedback strategies for route guidance in traffic networks, *Transportation Science*, **33**, 264–78.

Paz, A. & Peeta, S. (2009), Behavior-consistent real-time traffic routing under information provision, *Transportation Research Part C*, **17**(6), 642–61.

Putha, R., Quadrifoglio, L. & Zechman, E. (2012), Comparing ant colony optimization and genetic algorithm approaches for solving traffic signal coordination under oversaturation conditions, *Computer-Aided Civil and Infrastructure Engineering*, **27**(1), 14–28.

Samant, A. & Adeli, H. (2000), Feature extraction for traffic incident detection using wavelet transform and linear discriminant analysis, *Computer-Aided Civil and Infrastructure Engineering*, **15**(4), 241–50.

Samant, A. & Adeli, H. (2001), Enhancing neural network incident detection algorithms using wavelets, *Computer-Aided Civil and Infrastructure Engineering*, **16**(4), 239–45.

Sgambi, L., Gkoumas, K. & Bontempi, F. (2012), Genetic algorithms for the dependability assurance in the design of

a long span suspension bridge, *Computer-Aided Civil and Infrastructure Engineering*, **27**(9), 655–75.

Smadi, A., Baker, J. & Birst, S. (2006), Advantages of using innovative traffic data collection technologies, in *Proceedings of the 9th International Conference on Applications of Advanced Technology in Transportation*, 641–46.

Szeto, W. Y. & Sumalee, A. (2011), A cell-based model for multi-class doubly stochastic dynamic traffic assignment, *Computer-Aided Civil and Infrastructure Engineering*, **26**(8), 595–611.

Teklu, F., Sumalee, A. & Watling, D. (2007), A genetic algorithm for optimizing traffic control signals considering routing, *Computer-Aided Civil and Infrastructure Engineering*, **22**(1), 31–43.

Treiber, M., Kesting, A. & Wilson, R. E. (2011), Reconstructing the traffic state by fusion of heterogeneous data, *Computer-Aided Civil and Infrastructure Engineering*, **26**(6), 408–19.

Van den Berg, M., De Schutter, B., Hegyi, B. & Hellendoorn, J. (2001), Model predictive control for mixed urban and freeway networks. *Transportation Research Record*, **1748**, 55–65.

Wang, Y., Messmer, A. & Papageorgiou, M. (2001), Freeway network simulation and dynamic traffic assignment using METANET tools, *Transportation Research Record*, **1776**, 178–88.

Wang, Y. & Papageorgiou, M. (2000), Feedback routing control strategies for freeway networks: a comparative study, in *Proceedings of the 2nd International Conference on Traffic and Transportation Studies*, 642–49.

Wang, Y., Papageorgiou, M. & Messmer, A. (2002), A predictive feedback routing control strategy for freeway network traffic, in *Proceedings of American Control Conference*, 3606–11.

Wie, B., Tobin, R., Bernstein, D. & Friesz, T. (1995), Comparison of system optimum and user equilibrium dynamic traffic assignment with schedule delays, *Transportation Research*, **3C**, 389–11.

Wisten, M. B. & Smith, M. J. (1997), Distributed computation of dynamic traffic equilibria, *Transportation Research*, **5C**, 77–93.

Wu, J. & Chang, G. L. (1999), Heuristic method for optimal diversion control in freeway corridors, *Transportation Research Record*, **1667**, 8–15.